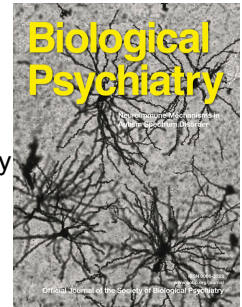


# Journal Pre-proof

Metabotropic glutamate receptor 5 in amygdala target neurons regulates susceptibility to chronic social stress

Jeongseop Kim, Shinwoo Kang, Tae-Yong Choi, Keun-A Chang, Ja Wook Koo



PII: S0006-3223(22)00028-2

DOI: <https://doi.org/10.1016/j.biopsych.2022.01.006>

Reference: BPS 14758

To appear in: *Biological Psychiatry*

Received Date: 29 March 2021

Revised Date: 10 January 2022

Accepted Date: 13 January 2022

Please cite this article as: Kim J., Kang S., Choi T.-Y., Chang K.-A & Koo J.W., Metabotropic glutamate receptor 5 in amygdala target neurons regulates susceptibility to chronic social stress, *Biological Psychiatry* (2022), doi: <https://doi.org/10.1016/j.biopsych.2022.01.006>.

This is a PDF file of an article that has undergone enhancements after acceptance, such as the addition of a cover page and metadata, and formatting for readability, but it is not yet the definitive version of record. This version will undergo additional copyediting, typesetting and review before it is published in its final form, but we are providing this version to give early visibility of the article. Please note that, during the production process, errors may be discovered which could affect the content, and all legal disclaimers that apply to the journal pertain.

© 2022 Published by Elsevier Inc on behalf of Society of Biological Psychiatry.

**Title: Metabotropic glutamate receptor 5 in amygdala target neurons regulates susceptibility to chronic social stress**

Jeongseop Kim<sup>1,2,\*</sup>, Shinwoo Kang<sup>3,4,5,6\*</sup>, Tae-Yong Choi<sup>1</sup>, Keun-A Chang<sup>3,4,5,¶</sup>, and Ja Wook Koo<sup>1,2,¶</sup>

**Affiliations**

<sup>1</sup>Emotion, Cognition & Behavior research group, Korea Brain Research Institute (KBRI), Dong-gu, Daegu 41062, Republic of Korea.

<sup>2</sup>Department of Brain and Cognitive Sciences, Daegu Gyeongbuk Institute of Science and Technology (DGIST), Dalseong-gun, Daegu 42988, Republic of Korea

<sup>3</sup>Department of Pharmacology, College of Medicine, Gachon University, Yeonsu-gu, Incheon 21936, Republic of Korea

<sup>4</sup>Neuroscience Research Institute, Gachon University, Namdong-gu, Incheon 21565, Republic of Korea

<sup>5</sup>Department of Health Sciences and Technology, GAIHST, Gachon University, Yeonsu-gu, Incheon 21999, Republic of Korea

<sup>6</sup>Department of Molecular Pharmacology and Experimental Therapeutics, Mayo Clinic, Rochester, Minnesota 55905, USA

<sup>\*,¶</sup> These authors contributed equally to this work.

**Contact Information**

Correspondence: keuna705@gachon.ac.kr (K.-A C), jawook.koo@kbri.re.kr (J.W.K)

**Short/Running title: Stress-resilient role of mGLUR5 in BLA target neurons**

**Keywords**

Metabotropic glutamate receptor 5, Basolateral amygdala, Medial prefrontal cortex, Ventral hippocampus, Stress resilience, Chronic social defeat stress, Depression

**Abstract**

**Background:** The metabotropic glutamate receptor 5 (mGluR5) has been implicated in stress-related psychiatric disorders, particularly major depressive disorders. Although growing evidence supports the pro-resilient role of mGluR5 in corticolimbic circuitry in the depressive-like behaviors following chronic stress exposure, the underlying neural mechanisms, including circuits and molecules, remain unknown.

**Methods:** We measured the c-fos<sup>+</sup> expression and probability of neurotransmitter release in and from the basolateral amygdala (BLA) neurons projecting to the medial prefrontal cortex (BLA→mPFC), and ventral hippocampus (BLA→vHPC) after chronic social defeat stress (CSDS). The role of the BLA projections in depressive-like behaviors was assessed using optogenetic manipulations, and the underlying molecular mechanisms of mGluR5 and downstream signaling were investigated by Western blotting, viral-mediated gene transfer, and pharmacological manipulations.

**Results:** CSDS disrupted the neural activity and glutamatergic transmission in both BLA→mPFC and BLA→vHPC projections. Optogenetic activation of the BLA projections reversed the detrimental CSDS effects on depressive-like behaviors and mGluR5 expression in mPFC and vHPC. Conversely, inhibition of the BLA projections of mice undergoing subthreshold social defeat stress-induced a susceptible phenotype and mGluR5 reduction.

These two BLA circuits appeared to act in an independent way. Importantly, we demonstrate that mGluR5 overexpression in mPFC or vHPC was pro-resilient, while the mGluR5 knockdown was pro-susceptible and that the pro-resilient effects of mGluR5 are mediated through distinctive downstream signaling pathways in the mPFC and vHPC.

**Conclusions:** These findings identify mGluR5 in the mPFC and vHPC that receive BLA inputs as a critical mediator of stress-resilience, highlighting circuit-specific signaling for depressive-like behaviors.

## Introduction

More than 300 million people worldwide, i.e., approximately 4.4% of the world's population, are estimated to have depression (1). Accumulating evidence suggests that stressful life events can increase the risk of developing depression (2,3). However, not all stress-exposed individuals develop stress-related psychiatric disorders, such as major depressive disorders (MDD), and some individuals are vulnerable to stress, while others maintain normal psychophysiological functioning (4,5).

It has been reported that the glutamatergic system in the brain regions such as basolateral amygdala (BLA), medial prefrontal cortex (mPFC), and hippocampus (HPC) plays a critical role in both stress susceptibility and resilience (6–8). The BLA is involved in emotional valence processing, both positive and negative (9,10). Recent studies have shown that distinct BLA cell populations are responsible for fear-, anxiety-, and/or depression-related behaviors via unique long-range projections to brain regions such as mPFC and ventral HPC (vHPC) (11–15). Deficits of the glutamate neurotransmitter system in these brain areas have been reported to be associated with chronic stress and depression (16,17).

In particular, dysfunctional mGluR5 signaling has been implicated in the pathophysiology of stress-related psychiatric disorders (18,19). Despite some inconsistencies (20,21), a large amount of evidence supports the pro-resilient role of mGluR5 in depressed patients. Previous neuroimaging studies have reported a decreased mGluR5 binding or glutamate metabolites in the PFC and HPC of depressed subjects (18,19,22). Reduced mGluR5 expression was also observed in the postmortem PFC of MDD patients (23). Genome-wide association studies and meta-analyses have also revealed reduced *Grm5* (encoding mGluR5) expression (24) in MDD

patients. Preclinical studies have shown that chronic corticosterone and stress downregulate mGluR5 expression and density in some brain regions, including the HPC (25–27). Consistently, mGluR5 knockout, particularly in the PFC glutamatergic neurons, promotes depressive-like behaviors (28,29).

Despite this evidence for a pro-resilient role of mGluR5, the underlying neural mechanisms, including circuits and molecules, are largely unknown in the context of chronic stress. In the current study, we investigated a presynaptic activity-dependent role of postsynaptic mGluR5 in molecular and behavioral responses to CSDS; an ethologically validated animal model of depression (30,31), with a focus on the projections from the BLA to the mPFC (BLA→mPFC) or to the vHPC (BLA→vHPC). Our results demonstrate that activation of the BLA projections and the activity-dependent mGluR5 signaling in the mPFC and vHPC affect depressive-like behaviors.

## Methods and Materials

### Animals

Eight-week-male C57BL/6NCrljOri mice (25–30 g, OrientBio, South Korea) and 3–8-month-old male CrlOri: CD-1 (35–45 g, OrientBio, South Korea) was used. Food and water were provided *ad libitum* during the acclimation period to the polycarbonate cage under a 12-h light/dark cycle. The temperature and humidity of the breeding room were maintained at 22 ± 2°C and 50 ± 10%. All experimental procedures followed the KBRI guidelines and Institutional Animal Care and Use Committee (M1-IACUC-19-0009).

## **Stress exposure and behavior test for depressive-like behaviors**

Chronic social defeat stress (CSDS) and subthreshold social defeat stress (SSDS) were conducted as described previously (32–34). For CSDS, each C57BL/6N mouse was exposed to 10 min of physical aggression by a CD-1 mouse. After the session, the defeated C57BL/6N mice were housed overnight within the same cage as the CD-1 mice, on the opposite side of a transparent and perforated divider to provide sensory, but not physical, contact. The procedure was repeated for 10 consecutive days with a new aggressor on each day. For SSDS, mice were exposed to three social defeat sessions: 5 min of physical defeat followed by 15 min with no defeat. All the stressed mice received the social interaction test (SIT) 24 h after the last defeat episodes and the sucrose preference test (SPT).

## **Viral injection**

Stereotaxic surgeries of viral injections were performed for the retrograde mapping of BLA→mPFC or BLA→vHPC PNs, *ex vivo* electrophysiological experiments, repeated optical activation/inactivation of BLA→mPFC and/or BLA→vHPC PNs, and localized *Grm5* gene overexpression or knockdown.

## **Cannula implantation and microinfusions**

Animals received bilateral intra-mPFC or vHPC infusions of 10 mM LY294002 (PI3K/AKT inhibitor, 1 µg/0.25 µL/side) or 25 mM U0126 (MAPK/ERK inhibitor, 1 µg/0.25 µL/side) at a continuous rate of 0.1 µL/min via a micro-infusion pump (Legato 200), around 15 min before SSDS.

**Ex vivo electrophysiology**

To assess paired-pulse ratio (PPR) of EPSC or IPSC, and AMPA/NMDA ratio, whole-cell-patch-clamp recordings were obtained from pyramidal neurons of the mPFC or vHPC in acute brain slices from mice that had been stereotactically injected with AAV5–Syn-ChrimsonR-tdTomato into the BLA.

**Data analysis**

We confirmed normality (Shapiro-Wilk test) and equal variance (Bartlett's test) on all data before a parametric analysis unless otherwise indicated. To assess differences between two experimental groups, Student *t*-tests, Student's *T*-tests with Welch's correction (for data sets with unequal variances), and Mann-Whitney *U*-tests (for non-normally distributed data) were used. For the analysis of three or more groups, one-way ANOVAs with Tukey's post hoc tests or with Welch's post hoc tests (for data sets with unequal variances) and the Kruskal-Wallis *H* test with Dunn's post hoc tests (for non-normally distributed data) were used. To analyse CSDS effects on the topographical distribution of activated BLA projections, two-way ANOVAs with Fisher's protected least significant difference (PLSD) post hoc tests were used. For details, please see supplemental methods and supplement table2.

**Additional Details.**

See supplemental methods for additional routine procedures and information including immunofluorescence, real-time qPCR, and Western immunoblot analysis.

## Results

### CSDS reduce cell activity in BLA projection neurons

We investigated whether c-Fos or other immediate early genes (IEGs), such as Arc and Egr-1, can be used as readouts for neural activity in the BLA neurons projecting to the mPFC (BLA→mPFC) or vHPC (BLA→vHPC). Two weeks after injection of AAVrg-hsyn-ChR2-EYFP or AAVrg-hsyn-Jaws-KGC-GFP-ER2 into the mPFC or vHPC (Figures S1A and S2A), each mouse received 5 min of photostimulation or photoinhibition over the BLA projection neurons (PNs) for a single day or 10 consecutive days without defeat stress exposure. A single day 5 min-optogenetic acute activation, but not acute inhibition, altered the expression of c-Fos, Arc, and Egr-1 at 90 min after optogenetic manipulation (Figures S1B-H). However, we could not observe acute optogenetic effects 24 h after acute photomanipulation (Figures S1I-O). As a result of a once-daily 5 min-optogenetic activation over BLA PNs for 10 consecutive days, we observed that c-Fos expression was increased both at 90 min (Figures S2B-H) and 24 h after the last optic manipulation compared to the control group (Figures S2I-O). In contrast, a 10 day-photoinhibition of BLA PNs decreased c-Fos expression at both time points. However, these chronic optogenetic effects were not explicit for Arc and Egr-1 expression. These observations support the use of c-Fos as an appropriate readout that reflects the rise and fall of chronic neural activity in both BLA→mPFC and BLA→vHPC PNs.

We then investigated whether CSDS affects the activation of BLA neurons projecting to the mPFC (BLA→mPFC) or vHPC (BLA→vHPC). We injected the retrograde adeno-associated virus (AAVrg)-hSyn-EGFP into the mPFC and AAVrg-hSyn-mCherry into the vHPC (Figure 1A). After 2 weeks of recovery, the mice received 10 days of CSDS. The social interaction

ratio was assessed in a social interaction test that proceeded 24 h after the last defeat. Animals were sacrificed 90 min after the behavioral tests for c-Fos immunolabeling, as described in previous studies (35,36). After triple-immunofluorescence labeling, the BLA tissues were imaged in at 4-6 anterior-posterior (AP) coordinates, and the retrogradely labeled BLA PN<sub>s</sub> were counted (Figure S3A). The BLA→mPFC PN<sub>s</sub> [EGFP<sup>+</sup> (green)/DAPI<sup>+</sup>] were present throughout the entire BLA with a highest density of around -1.6 mm AP from bregma. Conversely, BLA→vHPC PN<sub>s</sub> [mCherry<sup>+</sup>(red)/DAPI<sup>+</sup>] were preferentially located in the posterior part of the BLA (sparse around -1.0 mm AP from bregma and reaching a plateau around -1.6 mm AP), but with a smaller density across the entire BLA than BLA→mPFC PN<sub>s</sub> (Figures 1B, 1C, S3B).

Our retrograde localization and further analyses showed that CSDS had no effect on the relative cell numbers of BLA→mPFC (EGFP<sup>+</sup>/DAPI<sup>+</sup>), BLA→vHPC (mCherry<sup>+</sup>/DAPI<sup>+</sup>) PN<sub>s</sub>, or co-projecting BLA neurons (EGFP<sup>+</sup>/mCherry<sup>+</sup>/DAPI<sup>+</sup>) in the anterior (-1.1–1.3 mm AP), intermediate (-1.5–1.7 mm AP), to posterior sections (-1.9–2.1 mm AP) of the BLA (Figures S3C-F). Most importantly, despite null effect of CSDS on the overall number of c-Fos<sup>+</sup> cells [c-Fos<sup>+</sup>(white)/DAPI<sup>+</sup>, Figure S1G], the number of c-Fos<sup>+</sup> cells that were co-localized in the BLA→mPFC (c-Fos<sup>+</sup>/EGFP<sup>+</sup>/DAPI<sup>+</sup>) and/or BLA→vHPC (c-Fos<sup>+</sup>/mCherry<sup>+</sup>/DAPI<sup>+</sup>) circuits were decreased by CSDS compared to that in controls (Figures 1D, 1E, S3H-I). These data suggest that CSDS effects on cell activity are circuit-specific in the BLA. Additionally, we observed that both the BLA→mPFC or BLA→vHPC PN<sub>s</sub> were mostly colabeled with Ca<sup>2+</sup>/CaM-activated protein kinases (CamKIIα<sup>+</sup>, a glutamatergic marker; ~80%), but not with glutamate decarboxylase 67 (GAD67<sup>+</sup>, a GABAergic marker; 1–2%). These data indicate that the BLA PN<sub>s</sub> are mostly excitatory glutamatergic, rarely inhibitor GABAergic neurons, as

known in previous studies (37,38) (Figure S4). Taken together, these data suggest that CSDS may reduce the excitatory activity of the BLA→mPFC or BLA→vHPC PNs.

We directly assessed the effects of CSDS on circuit-specific glutamatergic synaptic transmission from the BLA, using *ex vivo* optogenetic patch-clamp electrophysiology. Two weeks after we injected AAV5-Syn-ChrimsonR-tdTomato into the BLA, the mice were exposed to CSDS for 10 days (Figures 1F, 1G, S5A). Then, synaptic transmissions were recorded in mPFC or vHPC neurons by activating ChrimsonR-expressing axon terminals from the BLA (Figures 1H, 1I, S5B). We found that CSDS significantly increased the paired-pulse ratio of the excitatory postsynaptic current (EPSC-PPR) in both BLA→mPFC (Figure 1J) and BLA→vHPC synapses (Figure 1K). However, the inhibitory postsynaptic current (IPSC)-PPR and AMPA/NMDA ratios were not altered (Figure S5B-S5F). These results suggest that CSDS decreases the glutamate release probability (39,40) at both BLA→mPFC and BLA→vHPC synapses.

### **Stimulation of BLA-projecting neurons rescues CSDS-induced social avoidance**

We then assessed the role of the BLA→mPFC and BLA→vHPC pathways in defeat-induced depressive-like behaviors by injecting AAV5-hSyn-hChR2-EYFP into the BLA (Figure 2A) and implanting optic fibers in the ChR2-infected axon terminals in the mPFC (Figure 2B) or vHPC (Figure 2D). Each mouse received 5 minutes of optic stimulation immediately after each defeat. CSDS significantly decreased social interaction with a target CD-1 mouse in control animals injected with AAV5-hSyn-EYFP, whereas BLA→mPFC photostimulation reversed the CSDS-induced social avoidance (Figure 2C). BLA→vHPC photostimulation also

attenuated the CSDS-induced social impairment (Figure 2E). These data indicate that the activation of BLA→mPFC or BLA→vHPC projections is pro-resilient in response to CSDS. To characterize the putative postsynaptic signaling events underlying the rescuing effects from photostimulation of the BLA projections on the CSDS-elicited social avoidance, we conducted qPCR for various glutamate receptor subunits in the mPFC and vHPC: metabotropic glutamate receptors (mGluRs), *Grm1*, *Grm2*, *Grm3*, *Grm4*, *Grm5*, *Grm6*, *Grm7*, and *Grm8*; subunits of N-methyl-D-aspartate receptors (NMDARs), *Grin1*, *Grin2a*, *Grin2b*, *Grin2c*, *Grin2d*, *Grin3a*, and *Grin3b*; subunits of  $\alpha$ -amino-3-hydroxy-5-methyl-4-isoxazole propionic acid receptors (AMPA receptors), *Gria1*, *Gria2*, *Gria3*, and *Gria4*; and subunits of kainic acid receptors (KARs), *Grik1*, *Grik2*, *Grik3*, *Grik4*, and *Grik5* (Figures S6 and S7). Among them, we found that *Grm5* was the only molecule in which an RNA expression was significantly decreased by CSDS but reversed by BLA→mPFC (Figure 2H) and BLA→vHPC stimulation (Figure 2K). Similar to the qPCR data, additional Western blot analyses showed similar expression patterns of mGluR5 proteins in the mPFC (Figures 2F and 2G) and vHPC (Figures 2I and 2J). These data suggest that mGluR5 expression in the mPFC and vHPC is modulated by BLA circuit activity.

### **Inhibition of BLA-projecting neurons has pro-depressive like effects**

To address whether inactivation of the BLA→mPFC and BLA→vHPC projections promotes vulnerability to defeat stress, in contrast to the pro-resilient effect by the photoactivation of the BLA projections, we injected AAV5-hSyn-eNpHR3.0-EYFP into BLA neurons (Figure 3A), and two weeks later, the optic fibers were implanted into the mPFC or vHPC (Figures 3B and 3D). The one-day subthreshold social defeat stress (SSDS) procedure did not reduce social

interactions, as observed in previous studies (34). However, mice that received photostimulation of amber light in the mPFC (Figure 3C) or vHPC (Figure 3E), immediately after each defeat, exhibited a sharp decrease in social interactions 24 h after the SSDS. Additionally, our data showed that the *Grm5* mRNA and mGluR5 protein expression was downregulated by SSDS with the photo-inactivation of BLA→mPFC (Figures 3F-H) or BLA→vHPC (Figures 3I-K) projections. These results indicate that the inactivation of the BLA→mPFC or BLA→vHPC circuits by SSDS promotes depressive-like behavioral abnormalities and reductions of mGluR5.

#### **Functional independence of the BLA projections in depressive-like behaviors**

Next, we investigated the interaction of the BLA projections in depressive-like behaviors in response to CSDS. For simultaneous photoactivation of the BLA→mPFC and BLA→vHPC projections, we injected AAV5-hSyn-hChR2-EYFP into the BLA and 2 weeks later, optic fibers were implanted in the mPFC and vHPC regions (Figures 4A, 4B). Each mouse received 5 min of ChR2 photoactivation immediately after each defeat. Interestingly, each photoactivation of BLA→mPFC and or BLA→vHPC projections successfully reversed CSDS-induced social avoidance (Figure 4C), anhedonic behavior, as measured in the sucrose preference test (SPT, Figure 4D). However, the simultaneous activation of these two BLA neural circuits did not further ameliorate the CSDS-induced depressive-like behaviors compared to the photoactivation of each BLA circuit, indicating no synergic effects. These results suggest that the BLA→mPFC and or BLA→vHPC projections play pro-resilient roles

in response to CSDS in an independent way despite of the BLA neurons co-projecting to the mPFC and vHPC, as in Figure S3F.

For cross-photomanipulations of the BLA→mPFC and BLA→vHPC circuits, we injected both the AAV5-hSyn-hChR2-EYFP and AAV5-hSyn-eNpHR3.0-EYFP into BLA, and 2 weeks later, optic fibers were implanted in the mPFC and vHPC (Figures 4E). Each mouse underwent a photoinactivation of the BLA→mPFC circuit and photoactivation of the BLA→vHPC circuits at the same time, immediately after receiving defeat (Figure 4F). The photostimulation of the BLA→vHPC circuits successfully blocked CSDS-induced social avoidance (Figure 4G), anhedonic behavior (Figure 4H), as in Figure 2E. However, the photoinhibition of the BLA→mPFC circuits did not aggravate the CSDS-induced social avoidance (Figure 4G), anhedonic behavior (Figure 4H), suggesting a possibility of the ceiling effect. However, the reversal effects of the BLA→vHPC PN photostimulation on the CSDS-induced depressive-like behaviors were also not affected by the BLA→mPFC PN photoinhibition. Likewise, the photostimulation of the BLA→ mPFC circuits reversed the CSDS-induced social avoidance (Figure 4J), as observed in Figure 2D. The reversal effects of the BLA→ mPFC PN photostimulation on the CSDS-induced depressive-like behaviors were also not affected by the BLA→ vHPC PN photoinhibition. Together, these data suggest the functional independence of these two BLA projections.

### **Pro-resilient role of mGluR5 in behavioral responses to CSDS**

To determine whether the mGluR5 has pro-resilient effects in response to CSDS, we first overexpressed mGluR5 by injecting lentivirus (LV)-EF1α-mGluR5-IRES-ZsGreen1 into the

mPFC and vHPC (Figures 5A, 5B, S8A, and S8C). When mice were evaluated for their social interaction 24 h after the last defeat, we observed that the mGluR5 overexpression in the mPFC and vHPC blunted CSDS-elicited social avoidance (Figures 5C, 5E) and anhedonic behavior (Figures 5D, 5F). These data suggest that mGluR5 has pro-resilient effects. Next, to investigate the causal link between mGluR5 expression and stress resilience, we examined whether a knockdown of mGluR5 expression in the mPFC or vHPC has pro-depressive effects. We injected AAV5-hSyn1-mGluR5-shRNA-GFP into the mPFC and vHPC (Figures 5G, 5H, S8B, and S8D). Two weeks later, the mice were exposed to SSDS. We found that mGluR5 knockdown in the mPFC or vHPC with SSDS significantly reduced social interaction (Figures 5I, 5K) and a sucrose preference (Figures 5J, 5L). Additionally, we investigated whether mGluR5 directly mediates the modulatory effects of the activity of the BLA projections on stress-related social avoidance behaviors by blocking the mGluR5 expression in the mPFC or vHPC and by photostimulating the BLA→mPFC or BLA→vHPC circuits (Figures S8E, S8F). Notably, mGluR5 knockdown target areas completely suppressed the reversal effects of a Chr2 activation of BLA→mPFC and BLA→vHPC projections on CSDS-elicited social avoidance (Figures S8G, S8H). Together, these results suggest a critical mediating role of mGluR5 in the BLA projection activities and stress-related social behaviors.

## **Pharmacological modulation of mGluR5 downstream signaling affects depressive-like behaviors**

Postsynaptic mGluR5 initiates a variety of downstream signaling pathways, mainly via the canonical  $G_q$ -dependent mechanism, generating inositol-1, 4, 5-trisphosphate, and

diacylglycerol, which typically activates protein kinase C (PKC). mGluR5-ERK coupling can occur via  $G_q$ -dependent mechanisms (' $G_q$ -PKC-ERK'), but also via  $G_q$ -independent (or Homer1b/c-dependent) mechanisms (41,42). Additionally, mGluR5 signaling can activate other pathways, such as the phosphatidylinositol 3-kinase (PI3K)/AKT/mammalian target of rapamycin kinase pathway through a  $G_q$ -independent mechanism ('Homer1b/c-PI3K-AKT') (43,44). Since a wide range of mGluR5 downstream signaling pathways can explain social avoidance, we next evaluated the activation and protein levels of several mGluR5 signaling components in the mPFC or vHPC using Western blot analyses. We observed reduced mGluR5 protein expression in both the mPFC and vHPC of susceptible (SUS), but not in resilient (RES) mice (Figures 6A-6D). Similarly, CSDS downregulated Homer1b/c expression and phosphorylation of AKT (pAKT) in the mPFC of SUS mice, but not in RES mice (Figures 6A-6D). No changes were observed in pPKC and pERK levels in the mPFC. By contrast, pPKC and pERK levels in the vHPC were decreased only in SUS animals (Figures 6A-6D). No changes were observed in Homer1b/c or pAKT in the vHPC. These findings suggest that differential mGluR5 downstream signaling in the mPFC and vHPC may mediate pro-resilient effects in response to CSDS. mGluR5 mediates the CSDS effects in a 'Homer1b/c-AKT' dependent way in the mPFC, whereas it mediates these effects in a ' $G_q$ -PKC-ERK' dependent manner in the vHPC. Next, we investigated whether each mGluR5 downstream signaling influences stress-related social behaviors. Approximately 2 weeks after the implantation of the cannula bilaterally in the mPFC and vHPC, we infused a selective PI3K-AKT inhibitor, LY294002, or a highly selective inhibitor of MAPK/ERK kinase, U0126, into the mPFC or vHPC. Social interaction was measured 24 h after the SSDS (Figures 6E, 6F). We found that the infusion of LY294002, but not of U0126, into the mPFC reduced social interaction (Figure

6G) and sucrose preference (Figure 6H), while the infusion of U0126, but not LY294002, into the vHPC decreased social interaction (Figure 6I) and a sucrose preference (Figure 6J). These data strongly suggest that the pro-resilient effects of mGluR5 signaling in the mPFC and vHPC are mediated through differential downstream signaling pathways: mGluR5-Homer1b/c-pAKT signaling pathways in the mPFC *vs.* mGluR5-G<sub>q</sub>-pERK signaling pathways in the vHPC (Figure S9).

## Discussion

This study provides evidence that mGluR5 in the mPFC and vHPC that is regulated by BLA outputs can be a molecular switch of susceptibility to resilience in response to CSDS. Our findings show that CSDS, an ethologically validated model of aspects of depression in mice (31), decreases the activity of BLA innervations to mPFC and vHPC, which is also observed in depressed patients (45,46). Optogenetic manipulation of the BLA projection activity to the mPFC or vHPC reversed CSDS-induced mGluR5 reduction and depressive-like behaviors as measured by social interaction and sucrose preference tests. Consistently, viral-mediated mGluR5 induction alleviated CSDS-induced social avoidance and anhedonia. Furthermore, we observed that selective blockade of the distinctive mGluR5 downstream signaling pathways attenuated CSDS-elicited depressive-like behaviors in a region-specific manner. Overall, our findings indicate that mGluR5 and its selective downstream signaling in the mPFC and vHPC, which are innervated by BLA projections, are pro-resilient in response to CSDS.

Although the BLA and its connections with other major limbic components such as the PFC and HPC have long been implicated in the regulation of emotion and etiology of stress-related

psychiatric diseases (47), there are only limited investigations on the roles of BLA projections in stress-related depressive-like behaviors. Consistent with our data, a recent study demonstrated that depressive behaviors induced by chronic immobilization stress were mediated by hypoactive glutamatergic neurons in the mPFC (48). Other studies have shown that stimulating BLA→vHPC circuits rescues depressive-like behaviors following repeated foot shock or chronic unpredictable mild stress, which weakens the BLA-vHPC connectivity (13,14). These findings highlight the pro-resilient role of the BLA→mPFC and BLA→vHPC projections in animal models of depression using chronic stress. Furthermore, our data in the present study suggest that these two BLA circuits that play the same pro-resilient role act in a functionally independent way: the pro-resilient effect of optogenetic stimulation over one of either BLA projection was not influenced by optogenetic manipulations (i.e., stimulation and inhibition) over the other BLA projection. Such functional independence for the same behavioral output might be associated with topographically different distributions or connectivity characteristics of BLA projection neurons, as observed in our study and others (49–52). However, it is noteworthy that the mPFC and vHPC give glutamatergic projections to the nucleus accumbens, which also receive projections from the BLA and other brain structures, forming a complex neural network for depressive-like behaviors (53–55). Thus, further investigation of putative interactions in this complex is required for a comprehensive understanding of the BLA circuitry functions in response to CSDS (57,59).

In the present study, the CSDS-induced hypoactivity of the BLA→mPFC and BLA→vHPC circuits and its concomitant depressive behaviors may occur through reductions in a glutamate release at BLA→mPFC or BLA→vHPC synapses, assessed by PPRs of the EPSC following pathway-specific stimulation. Our findings are in line with earlier preclinical evidence showing

that glutamine supplementation reverses reduced levels of glutamate/glutamine cycling or glutamatergic activity in the PFC of chronically stressed mice, thereby attenuating stress-induced depressive-like behaviors (48,56,58). Clinical studies have also shown reduced glutamate metabolite levels in the PFC and HPC of depressed patients (60,61). This suggests a critical role of glutamatergic transmission at the BLA terminals in depressive-like behaviors.

It is worth noting that mGluR5 is the only glutamate receptor subtype whose expression is decreased by CSDS and reversed by the stimulation of BLA projections. The expression of glutamate receptors such as *Grin2a*, *Gria1*, *Gria2*, *Gria3*, and/or *Gria4* was also reduced in the mPFC and vHPC of stressed mice, but the BLA activation had no reversal effects. These data suggest that mGluR5 in the BLA-PN targets, such as mPFC and vHPC, is the only receptor that can regulate the detrimental effects of CSDS on depressive-like behaviors in a BLA-PN activity-dependent manner. Indeed, such mGluR5 alterations were compatible with social avoidance and anhedonic behaviors that were induced by CSDS but reversed by BLA circuit stimulation. Consistently, we found a regulatory effect of viral-mediated mGluR5 induction in the mPFC and vHPC on CSDS-induced depressive-like behaviors.

We further observed that the mGluR5 knockdown in both the mPFC and vHPC completely blocked the reversal effects from photoactivation of the BLA projections on CSDS-induced depressive-like behavior. This supports a scheme wherein mGluR5 is a key mediator of the pro-resilient effects of the BLA circuit activation on depressive-like behaviors in response to CSDS. It is of particular interest that the resilient effects of mGluR5 are distinctively mediated by ‘G<sub>q</sub>-independent Homer1b/c-AKT’ signaling in the mPFC and by ‘G<sub>q</sub>-dependent PKC-ERK’ signaling in the vHPC. These data are not consistent with previous studies showing enhanced

mGluR5 and Homer1b/c expressions in the dorsal hippocampus of CSDS-susceptible mice (62,63). This could be due to differences in connectivity-based functions in the dorsal HPC, which primarily performs cognitive functions, and in the vHPC, which performs functions related to stress and emotion (64).

In conclusion, our study demonstrates a pro-resilient role of mGluR5 signaling in the mPFC and vHPC innervated by BLA in social behaviors affected by CSDS. The sustained inactivation of BLA-projecting neurons, in the context of stress, suppresses postsynaptic mGluR5, which may produce pathological effects, as observed in depressed patients (19). However, the pro-resilient mGluR5 signaling in the BLA outputs is likely in contrast to the antidepressant effects of mGluR5 antagonists or mGluR5 deletion (20,65). These inconsistencies may be due to the diverse roles of mGluR5 in specific neuronal populations, regions, and circuits, which are differentially modulated by various stresses (29,66,67), and requires further study. Sex-specific physiological characteristics of mGluR5 in depression also need to be further investigated. It may be difficult to explore this system in female depressed subjects because of the more noticeable circadian variation of mGluR5 availability in females and circadian misalignment in depressed subjects (18,68,69). However, such an investigation would be a crucial step towards the development or optimization of precision interventions to treat depression, especially for women, who show a higher lifetime prevalence of depression than men (70,71).

#### **Acknowledgments and Disclosures**

We thank Chul Hoon Kim (Yonsei University College of Medicine) for providing the Lentiviral vectors, and Tae-Eun Kim (KBRI and DGIST), Yoo Jin Lee (KBRI), Hyang-Sook

Hoe (KBRI) for their technical support. This work was supported by the National Research Foundation of Korea (NRF) (2016M3C7A1914451, and 2020M3A9E4104384 to K.-A C. and 2017M3C7A1048089, and 2018M3C7A1024150 to J.W.K.) and the KBRI Basic Research Program (21-BR-02-06 to J.W.K.).

J.K., S.K., T-Y.C., K.-A C., and J.W.K. jointly conceived and designed the study. J.K and S.K performed the Chr2, NpHR, Jaws, Lenti, shRNA virus surgery, histological analysis, social interaction tests, and analyzed the data. J.K. and S.K. performed CSDS and optogenetics. J.K performed SSDS, FST, SPT, real-time RT-PCR, and drug cannula infusion. T-Y.C performed the electrophysiological experiments. J.K. and S.K. collected tissue samples and performed RT-PCR and Western blotting, respectively. J.K., S.K., K.-A C., and J.W.K. wrote the manuscript. All authors discussed and commented on the manuscript and approved the final submission.

The authors report no biomedical financial interests or potential conflicts of interest.

## References

1. James SL, Abate D, Abate KH, Abay SM, Abbafati C, Abbasi N, *et al.* (2018): Global, regional, and national incidence, prevalence, and years lived with disability for 354 diseases and injuries for 195 countries and territories, 1990–2017: a systematic analysis for the Global Burden of Disease Study 2017. *Lancet* 392: 1789–1858.
2. Kessler RC (1997): THE EFFECTS OF STRESSFUL LIFE EVENTS ON DEPRESSION. *Annu Rev Psychol* 48: 191–214.
3. Kendler KS, Karkowski LM, Prescott CA (1999): Causal relationship between stressful life events and the onset of major depression. *Am J Psychiatry* 156: 837–841.
4. Feder A, Nestler EJ, Charney DS (2009): Psychobiology and molecular genetics of resilience. *Nat Rev Neurosci* 10: 446–457.
5. Han M-H, Nestler EJ (2017): Neural Substrates of Depression and Resilience. *Neurother J Am Soc Exp Neurother* 14: 677–686.
6. Reus\* GZ, Moura AB de, Silva RH, Quevedo WRR and J (2018): Resilience Dysregulation in Major Depressive Disorder: Focus on Glutamatergic Imbalance and Microglial Activation. *Current Neuropsychopharmacology*, vol. 16. pp 297–307.
7. McEwen BS, Gray J, Nasca C (2015): Recognizing Resilience: Learning from the Effects of Stress on the Brain. *Neurobiol Stress* 1: 1–11.
8. Zhang W-H, Zhang J-Y, Holmes A, Pan B-X (2021): Amygdala Circuit Substrates for Stress Adaptation and Adversity. *Biol Psychiatry* 89: 847–856.

9. Tye KM (2018): Neural Circuit Motifs in Valence Processing. *Neuron* 100: 436–452.
10. O'Neill P-K, Gore F, Salzman CD (2018): Basolateral amygdala circuitry in positive and negative valence. *Curr Opin Neurobiol* 49: 175–183.
11. Felix-Ortiz AC, Tye KM (2014): Amygdala Inputs to the Ventral Hippocampus Bidirectionally Modulate Social Behavior. *J Neurosci* 34: 586 LP – 595.
12. Liu W-Z, Zhang W-H, Zheng Z-H, Zou J-X, Liu X-X, Huang S-H, *et al.* (2020): Identification of a prefrontal cortex-to-amygdala pathway for chronic stress-induced anxiety. *Nat Commun* 11: 2221.
13. Ma H, Li C, Wang J, Zhang X, Li M, Zhang R, *et al.* (2021): Amygdala-hippocampal innervation modulates stress-induced depressive-like behaviors through AMPA receptors. *Proc Natl Acad Sci* 118: e2019409118.
14. Yang Y, Wang Z-H, Jin S, Gao D, Liu N, Chen S-P, *et al.* (2016): Opposite monosynaptic scaling of BLP–vCA1 inputs governs hopefulness- and helplessness-modulated spatial learning and memory. *Nat Commun* 7: 11935.
15. Burgos-Robles A, Kimchi EY, Izadmehr EM, Porzenheim MJ, Ramos-Guasp WA, Nieh EH, *et al.* (2017): Amygdala inputs to prefrontal cortex guide behavior amid conflicting cues of reward and punishment. *Nat Neurosci* 20: 824–835.
16. Duman RS, Sanacora G, Krystal JH (2019): Altered Connectivity in Depression: GABA and Glutamate Neurotransmitter Deficits and Reversal by Novel Treatments. *Neuron* 102: 75–90.

17. Lener MS, Niciu MJ, Ballard ED, Park M, Park LT, Nugent AC, Zarate CAJ (2017):  
Glutamate and Gamma-Aminobutyric Acid Systems in the Pathophysiology of Major  
Depression and Antidepressant Response to Ketamine. *Biol Psychiatry* 81: 886–897.
18. Esterlis I, Holmes SE, Sharma P, Krystal JH, DeLorenzo C (2018): Metabotropic  
Glutamatergic Receptor 5 and Stress Disorders: Knowledge Gained From Receptor  
Imaging Studies. *Biol Psychiatry* 84: 95–105.
19. Terbeck S, Akkus F, Chesterman LP, Hasler G (2015): The role of metabotropic  
glutamate receptor 5 in the pathogenesis of mood disorders and addiction: combining  
preclinical evidence with human Positron Emission Tomography (PET) studies. *Front  
Neurosci* 9: 86.
20. Krystal JH, Mathew SJ, D’Souza DC, Garakani A, Gunduz-Bruce H, Charney DS (2010):  
Potential psychiatric applications of metabotropic glutamate receptor agonists and  
antagonists. *CNS Drugs* 24: 669–693.
21. Abdallah CG, Hannestad J, Mason GF, Holmes SE, DellaGioia N, Sanacora G, *et al.*  
(2017): Metabotropic Glutamate Receptor 5 and Glutamate Involvement in Major  
Depressive Disorder: A Multimodal Imaging Study. *Biol psychiatry Cogn Neurosci  
neuroimaging* 2: 449–456.
22. Kim J-H, Joo Y-H, Son Y-D, Kim J-H, Kim Y-K, Kim H-K, *et al.* (2019): In vivo  
metabotropic glutamate receptor 5 availability-associated functional connectivity  
alterations in drug-naïve young adults with major depression. *Eur  
Neuropsychopharmacol J Eur Coll Neuropsychopharmacol* 29: 278–290.

23. Deschwanden A, Karolewicz B, Feyissa AM, Treyer V, Ametamey SM, Johayem A, *et al.* (2011): Reduced metabotropic glutamate receptor 5 density in major depression determined by [(11)C]ABP688 PET and postmortem study. *Am J Psychiatry* 168: 727–734.
24. Howard DM, Adams MJ, Shirali M, Clarke T-K, Marioni RE, Davies G, *et al.* (2018): Genome-wide association study of depression phenotypes in UK Biobank identifies variants in excitatory synaptic pathways. *Nat Commun* 9: 1470.
25. Iyo AH, Feyissa AM, Chandran A, Austin MC, Regunathan S, Karolewicz B (2010): Chronic corticosterone administration down-regulates metabotropic glutamate receptor 5 protein expression in the rat hippocampus. *Neuroscience* 169: 1567–1574.
26. Wierońska J, Brański P, Szewczyk B, Palucha-Poniewiera A, Papp M, Gruca P, *et al.* (2001): Changes in the expression of metabotropic glutamate receptor 5 (mGluR5) in the rat hippocampus in an animal model of depression. *Pol J Pharmacol* 53: 659–662.
27. Kovačević T, Skelin I, Minuzzi L, Rosa-Neto P, Diksic M (2012): Reduced metabotropic glutamate receptor 5 in the Flinders Sensitive Line of rats, an animal model of depression: an autoradiographic study, 2012/01/31. *Brain Res Bull* 87: 406–412.
28. Shin S, Kwon O, Kang JI, Kwon S, Oh S, Choi J, *et al.* (2015): mGluR5 in the nucleus accumbens is critical for promoting resilience to chronic stress. *Nat Neurosci* 18: 1017–1024.
29. Lee K-W, Westin L, Kim J, Chang JC, Oh Y-S, Amreen B, *et al.* (2015): Alteration by p11 of mGluR5 localization regulates depression-like behaviors. *Mol Psychiatry* 20:

1546–1556.

30. Krishnan V, Han M-H, Graham DL, Berton O, Renthal W, Russo SJ, *et al.* (2007):

Molecular Adaptations Underlying Susceptibility and Resistance to Social Defeat in  
Brain Reward Regions. *Cell* 131: 391–404.

31. Krishnan V, Nestler EJ (2011): Animal models of depression: molecular perspectives.

*Curr Top Behav Neurosci* 7: 121–147.

32. Wook Koo J, Labonté B, Engmann O, Calipari ES, Juarez B, Lorsch Z, *et al.* (2016):

Essential Role of Mesolimbic Brain-Derived Neurotrophic Factor in Chronic Social  
Stress-Induced Depressive Behaviors. *Biol Psychiatry* 80: 469–478.

33. Walsh JJ, Friedman AK, Sun H, Heller EA, Ku SM, Juarez B, *et al.* (2014): Stress and

CRF gate neural activation of BDNF in the mesolimbic reward pathway. *Nat Neurosci*  
17: 27–29.

34. Chaudhury D, Walsh JJ, Friedman AK, Juarez B, Ku SM, Koo JW, *et al.* (2013): Rapid

regulation of depression-related behaviours by control of midbrain dopamine neurons.  
*Nature* 493: 532–536.

35. Barth AL, Gerkin RC, Dean KL (2004): Alteration of neuronal firing properties after in

vivo experience in a FosGFP transgenic mouse. *J Neurosci* 24: 6466–6475.

36. Morgan JJ, Cohen DR, Hempstead JL, Curran T (1987): Mapping patterns of c-fos

expression in the central nervous system after seizure. *Science* (80- ) 237: 192 LP – 197.

37. Goldstein L (1992): The Amygdala: Neurobiological Aspects of Emotion, Memory, and

Mental Dysfunction. *Yale J Biol Med* 65: 540–542.

38. Liu J, Hu T, Zhang M-Q, Xu C-Y, Yuan M-Y, Li R-X (2021): Differential efferent projections of GABAergic neurons in the basolateral and central nucleus of amygdala in mice. *Neurosci Lett* 745: 135621.
39. Manabe T, Wyllie DJ, Perkel DJ, Nicoll RA (1993): Modulation of synaptic transmission and long-term potentiation: effects on paired pulse facilitation and EPSC variance in the CA1 region of the hippocampus. *J Neurophysiol* 70: 1451–1459.
40. Dobrunz LE, Stevens CF (1997): Heterogeneity of release probability, facilitation, and depletion at central synapses. *Neuron* 18: 995–1008.
41. Mao L, Yang L, Tang Q, Samdani S, Zhang G, Wang JQ (2005): The Scaffold Protein Homer1b/c Links Metabotropic Glutamate Receptor 5 to Extracellular Signal-Regulated Protein Kinase Cascades in Neurons. *J Neurosci* 25: 2741 LP – 2752.
42. Stoppel LJ, Auerbach BD, Senter RK, Preza AR, Lefkowitz RJ, Bear MF (2017):  $\beta$ -Arrestin2 Couples Metabotropic Glutamate Receptor 5 to Neuronal Protein Synthesis and Is a Potential Target to Treat Fragile X. *Cell Rep* 18: 2807–2814.
43. Olmo IG, Ferreira-Vieira TH, Ribeiro FM (2016): Dissecting the Signaling Pathways Involved in the Crosstalk between Metabotropic Glutamate 5 and Cannabinoid Type 1 Receptors. *Mol Pharmacol* 90: 609 LP – 619.
44. Holz A, Mülsch F, Schwarz MK, Hollmann M, Döbrössy MD, Coenen VA, *et al.* (2019): Enhanced mGlu5 Signaling in Excitatory Neurons Promotes Rapid Antidepressant Effects via AMPA Receptor Activation. *Neuron* 104: 338-352.e7.

45. Tang Y, Kong L, Wu F, Womer F, Jiang W, Cao Y, *et al.* (2013): Decreased functional connectivity between the amygdala and the left ventral prefrontal cortex in treatment-naïve patients with major depressive disorder: a resting-state functional magnetic resonance imaging study. *Psychol Med* 43: 1921–1927.
46. Cullen KR, Westlund MK, Klimes-Dougan B, Mueller BA, Houry A, Eberly LE, Lim KO (2014): Abnormal amygdala resting-state functional connectivity in adolescent depression. *JAMA psychiatry* 71: 1138–1147.
47. Ulrich-Lai YM, Herman JP (2009): Neural regulation of endocrine and autonomic stress responses. *Nat Rev Neurosci* 10: 397–409.
48. Son H, Baek JH, Go BS, Jung D-H, Sontakke SB, Chung HJ, *et al.* (2018): Glutamine has antidepressive effects through increments of glutamate and glutamine levels and glutamatergic activity in the medial prefrontal cortex. *Neuropharmacology* 143: 143–152.
49. McGarry LM, Carter AG (2017): Prefrontal Cortex Drives Distinct Projection Neurons in the Basolateral Amygdala. *Cell Rep* 21: 1426–1433.
50. Hintiryan H, Bowman I, Johnson DL, Korobkova L, Zhu M, Khanjani N, *et al.* (2021): Connectivity characterization of the mouse basolateral amygdalar complex. *Nat Commun* 12: 2859.
51. Beyeler A, Chang C-J, Silvestre M, Lévesque C, Namburi P, Wildes CP, Tye KM (2018): Organization of Valence-Encoding and Projection-Defined Neurons in the Basolateral Amygdala. *Cell Rep* 22: 905–918.

52. Pi G, Gao D, Wu D, Wang Y, Lei H, Zeng W, *et al.* (2020): Posterior basolateral amygdala to ventral hippocampal CA1 drives approach behaviour to exert an anxiolytic effect. *Nat Commun* 11: 183.
53. Bagot RC, Parise EM, Peña CJ, Zhang H-X, Maze I, Chaudhury D, *et al.* (2015): Ventral hippocampal afferents to the nucleus accumbens regulate susceptibility to depression. *Nat Commun* 6: 7062.
54. Nestler EJ (2015): Chapter Six - Role of the Brain's Reward Circuitry in Depression: Transcriptional Mechanisms. In: De Biasi MBT-IR of N, editor. *Nicotine Use in Mental Illness and Neurological Disorders*, vol. 124. Academic Press, pp 151–170.
55. Dieterich A, Floeder J, Stech K, Lee J, Srivastava P, Barker DJ, Samuels BA (2021): Activation of Basolateral Amygdala to Nucleus Accumbens Projection Neurons Attenuates Chronic Corticosterone-Induced Behavioral Deficits in Male Mice. *Front Behav Neurosci* 15: 643272.
56. Banasr M, Chowdhury GMI, Terwilliger R, Newton SS, Duman RS, Behar KL, Sanacora G (2010): Glial pathology in an animal model of depression: reversal of stress-induced cellular, metabolic and behavioral deficits by the glutamate-modulating drug riluzole. *Mol Psychiatry* 15: 501–511.
57. Muir J, Lopez J, Bagot RC (2019): Wiring the depressed brain: optogenetic and chemogenetic circuit interrogation in animal models of depression. *Neuropsychopharmacol Off Publ Am Coll Neuropsychopharmacol* 44: 1013–1026.
58. Baek JH, Vignesh A, Son H, Lee DH, Roh GS, Kang SS, *et al.* (2019): Glutamine

Supplementation Ameliorates Chronic Stress-induced Reductions in Glutamate and  
Glutamine Transporters in the Mouse Prefrontal Cortex, 2019/04/30. *Exp Neurobiol* 28:  
270–278.

59. Knowland D, Lim BK (2018): Circuit-based frameworks of depressive behaviors: The  
role of reward circuitry and beyond. *Pharmacol Biochem Behav* 174: 42–52.

60. Hasler G, van der Veen JW, Tumonis T, Meyers N, Shen J, Drevets WC (2007): Reduced  
prefrontal glutamate/glutamine and gamma-aminobutyric acid levels in major  
depression determined using proton magnetic resonance spectroscopy. *Arch Gen  
Psychiatry* 64: 193–200.

61. Block W, Träber F, von Widdern O, Metten M, Schild H, Maier W, *et al.* (2009): Proton  
MR spectroscopy of the hippocampus at 3 T in patients with unipolar major depressive  
disorder: correlates and predictors of treatment response. *Int J Neuropsychopharmacol*  
12: 415–422.

62. Wagner K V, Hartmann J, Labermaier C, Häusl AS, Zhao G, Harbich D, *et al.* (2015):  
Homer1/mGluR5 activity moderates vulnerability to chronic social stress.  
*Neuropsychopharmacol Off Publ Am Coll Neuropsychopharmacol* 40: 1222–1233.

63. Li M-X, Li Q, Sun X-J, Luo C, Li Y, Wang Y-N, *et al.* (2019): Increased Homer1-  
mGluR5 mediates chronic stress-induced depressive-like behaviors and glutamatergic  
dysregulation via activation of PERK-eIF2 $\alpha$ . *Prog Neuropsychopharmacol Biol  
Psychiatry* 95: 109682.

64. Fanselow MS, Dong H-W (2010): Are the dorsal and ventral hippocampus functionally

distinct structures? *Neuron* 65: 7–19.

65. Pilc A, Chaki S, Nowak G, Witkin JM (2008): Mood disorders: regulation by metabotropic glutamate receptors. *Biochem Pharmacol* 75: 997–1006.

66. Lowery-Gionta EG, Crowley NA, Bukalo O, Silverstein S, Holmes A, Kash TL (2018): Chronic stress dysregulates amygdalar output to the prefrontal cortex. *Neuropharmacology* 139: 68–75.

67. Zhang J-Y, Liu T-H, He Y, Pan H-Q, Zhang W-H, Yin X-P, *et al.* (2019): Chronic Stress Remodels Synapses in an Amygdala Circuit-Specific Manner. *Biol Psychiatry* 85: 189–201.

68. DeLorenzo C, Gallezot J-D, Gardus J, Yang J, Planeta B, Nabulsi N, *et al.* (2017): In vivo variation in same-day estimates of metabotropic glutamate receptor subtype 5 binding using [(11)C]ABP688 and [(18)F]FPEB. *J Cereb blood flow Metab Off J Int Soc Cereb Blood Flow Metab* 37: 2716–2727.

69. Elmenhorst D, Mertens K, Kroll T, Oskamp A, Ermert J, Elmenhorst E-M, *et al.* (2016): Circadian variation of metabotropic glutamate receptor 5 availability in the rat brain. *J Sleep Res* 25: 754–761.

70. Cyranowski JM, Frank E, Young E, Shear MK (2000): Adolescent onset of the gender difference in lifetime rates of major depression: a theoretical model. *Arch Gen Psychiatry* 57: 21–27.

71. Albert PR (2015, July): Why is depression more prevalent in women? *Journal of Psychiatry & Neuroscience : JPN*, vol. 40. pp 219–221.

## Figure Legends

### Figure 1. CSDS effects on cell activation and synaptic function in BLA neurons projecting to the mPFC or vHPC

(A) Schematic of AAVrg-hSyn-EGFP injection into the mPFC and AAVrg-hSyn-mCherry into the vHPC, and confocal images showing injection sites. Scale bars, 1 mm. (B-C) Representative confocal images show c-Fos<sup>+</sup> (blue), BLA→mPFC projecting neurons (PNs) (green), and BLA→vHPC PNs (red) in the BLA. Scale bars, 50 μm (B) and 5 μm (C). (D-E) c-Fos<sup>+</sup> BLA→mPFC PNs (blue + green, arrows in B, unpaired *t*-test,  $t_8 = 2.896$ ,  $p = 0.0200$ ,  $n = 5$ ) or c-Fos<sup>+</sup> BLA→vHPC PNs (blue + red, arrowheads in B, unpaired *t*-test,  $t_8 = 5.661$ ,  $p = 0.0005$ ,  $n = 5$ ) were decreased in the intermediate part of BLA (-1.5 to -1.7 mm AP from the bregma) in CSDS compared with control (CTRL) mice. For the CSDS effects on distribution of the c-Fos<sup>+</sup> BLA PNs at the anterior (-1.1 to -1.3 mm AP) or posterior BLA (-1.9 to -2.1 mm AP) please see Figures S1H and S1I. (F-G) Experimental procedures for *ex vivo* electrophysiology using AAV5-Syn-ChrimsonR-tdTomato infusion into the BLA. Scale bar, 1000 μm. (H-I) Representative EPSC-PPR evoked by photostimulation of axon terminals from the BLA into the mPFC (H) and vHPC (I). Red squares indicate light pulse delivery. Scale bars = 1 mm. (J-K) EPSC-PPR was increased in BLA→mPFC synapses (J, unpaired *t*-test,  $t_{17} = 4.508$ ,  $p = 0.0003$ ,  $n = 18, 20$ ) and in BLA→vHPC synapses (K, Welch's *t* test,  $t_{31.45} = 2.816$ ,  $p = 0.0083$ ,  $n = 23, 20$ ) of CSDS mice. Student's *t* test (unpaired), \* $p < 0.05$ , \*\* $p < 0.01$ , \*\*\* $p < 0.001$ , \*\*\*\* $p < 0.0001$ . Data represented as mean ± SEM.

**Figure 2. Activation of BLA projections in social behaviors and mGluR5 expression in response to CSDS**

(A) Experimental procedures for ChR2 stimulation of the BLA→mPFC or BLA→vHPC pathways. (B, D) AAV5-hSyn-hChR2(H134R)-EYFP was injected into the BLA, and optic fibers were implanted into the mPFC or vHPC. Scale bars, 500  $\mu$ m. (C, E) Photoactivation of the BLA→mPFC circuit significantly reversed social avoidance by CSDS (one-way ANOVA with Welch's test,  $F_{2, 33.47} = 8.663$ ,  $p = 0.0009$ ,  $n = 14, 24, 20$ ). BLA→vHPC photoactivation also prevented the social avoidance by CSDS (one-way ANOVA with Welch's test,  $F_{2, 33.47} = 6.801$ ,  $p = 0.0047$ ,  $n = 14, 19, 21$ ). (F, G) Typical immunoblots with quantification for mGluR5 protein expression in the mPFC of EYFP+Stress naïve, EYFP+CSDS, and ChR2+CSDS mice. EYFP+CSDS mice showed reduced mGluR5 protein expression, which was blocked by BLA→mPFC activation during CSDS (ChR2+CSDS) (one-way ANOVA with Tukey's test,  $F_{2, 12} = 18.26$ ,  $p = 0.0002$ ,  $n = 5$ ). (H) Consistently, CSDS decreased *Grm5* mRNA expression, which was rescued by the BLA→mPFC activation (one-way ANOVA with Welch's test,  $F_{2, 7.595} = 21.34$ ,  $p = 0.0008$ ,  $n = 5$ ). (I, J) Similarly to the mPFC, reduced levels of mGluR5 proteins in the vHPC by CSDS were alleviated by BLA→vHPC activation during CSDS (one-way ANOVA with Tukey's test,  $F_{2, 12} = 19.56$ ,  $p = 0.0002$ ,  $n = 5$ ). (K) *Grm5* mRNA levels also decreased following CSDS, whose effects were blocked by BLA→vHPC activation (one-way ANOVA with Welch's test,  $F_{2, 6.149} = 13.32$ ,  $p = 0.0058$ ,  $n = 5$ ). Post hoc analysis,  $*p < 0.05$ ,  $**p < 0.01$ ,  $***p < 0.001$ ,  $****p < 0.0001$  compared to control+EYFP group;  $^{\#}p < 0.05$ ,  $^{\#\#}p < 0.01$ ,  $^{\#\#\#}p < 0.001$  compared to CSDS+EYFP group. Data represented as mean  $\pm$  SEM.

**Figure 3. Inactivation of BLA projections in social behaviors and mGluR5 expression in response to CSDS**

(A) Experimental procedures for photo-inactivation of the BLA→mPFC or BLA→vHPC pathways in SSDS. (B, D) For photo-inactivation, AAV5-hSyn-eNpHR3.0-EYFP was infused into the BLA and 594-nm of constant amber light was delivered into the mPFC (C) or vHPC (E). Scale bars, 250  $\mu$ m. (C) Photo-inactivation of the BLA→mPFC circuit significantly reduced the social interaction during the SSDS procedure (Kruskal Wallis H test,  $H = 10.90$ ,  $p = 0.0013$ ,  $n = 7, 7, 6$ ). (E) BLA→vHPC photo-inactivation also significantly induced susceptibility to SSDS (one-way ANOVA with Welch's test,  $F_{2, 9.238} = 6.404$ ,  $p = 0.0180$ ,  $n = 7, 6, 9$ ). (F, G) SSDS did not alter mGluR5 protein expression in the mPFC, which was decreased by BLA→mPFC inactivation (one-way ANOVA with Tukey's test,  $F_{2, 12} = 35.36$ ,  $p < 0.0001$ ,  $n = 5$ ). (H) *Grm5* mRNA levels in the mPFC were also reduced by BLA→mPFC inactivation during the SSDS procedure (one-way ANOVA with Tukey's test,  $F_{2, 13} = 35.36$ ,  $p = 0.0099$ ,  $n = 6, 5, 5$ ). (I, J, K) Similarly to the mPFC, vHPC mGluR5 protein and mRNA levels were not changed by SSDS, but decreased by the BLA→vHPC inactivation during the SSDS (J, protein: one-way ANOVA with Tukey's test,  $F_{2, 12} = 19.56$ ,  $p = 0.0002$ ,  $n = 5$ ; K, mRNA:  $F_{2, 14} = 5.471$ ,  $p = 0.0175$ ,  $n = 6, 6, 5$ ). Post hoc analysis,  $*p < 0.05$ ,  $**p < 0.01$ ,  $****p < 0.0001$  compared to control+EYFP group;  $^{\#}p < 0.05$ ,  $^{\#\#}p < 0.01$ ,  $^{\#\#\#}p < 0.001$  compared to SSDS+EYFP group. Data represented as mean  $\pm$  SEM.

**Figure 4. Null interaction of BLA projections in depressive-like behaviors in response to CSDS**

(A) Experimental procedures for simultaneous photoactivation of BLA→mPFC and BLA→vHPC pathways in CSDS. (B) AAV5-hSyn-hChR2(H134R)-EYFP was injected into the BLA, and optic fibers were implanted into both the mPFC and vHPC. Scale bars, 500  $\mu$ m. (C, D) Photoactivation of the BLA→mPFC and/or BLA→vHPC circuits significantly reversed CSDS-induced social avoidance (C, Kruskal Wallis H test,  $H = 28$ ,  $p = 0.0003$ ,  $n = 9, 10, 6, 6$ , 6) and anhedonic behavior, which was measured by sucrose preference test (D, one-way ANOVA with Tukey's test,  $F_{4, 35} = 6.527$ ,  $p = 0.0005$ ,  $n = 10, 10, 7, 7, 6$ ). Of note, the photoactivation effects of either of the BLA pathways were not different from the simultaneous photoactivation effects of both the BLA pathways, suggesting null synergic interaction of those BLA circuits on depressive-like behaviors. (E) Experimental procedures for cross-photomanipulation of BLA→mPFC and BLA→vHPC pathways in CSDS. (F, I) After AAV5-hSyn-hChR2(H134R)-EYFP and AAV5-hSyn-eNpHR3.0-EYFP were injected into the BLA, we implanted optic fibers for photoinhibition into the mPFC and those for photoactivation into the vHPC, and *vice versa*. Scale bars, 500  $\mu$ m. (G, H) CSDS-induced social avoidance and anhedonic behavior were not aggravated by NpHR photo-inactivation over BLA→mPFC circuit, but reversed by ChR2 activation over BLA→vHPC circuit (G, social interaction, one-way ANOVA with Tukey's test,  $F_{4, 32} = 10.39$ ,  $p < 0.0001$ ,  $n = 8, 10, 6, 7, 6$ ; H, sucrose preference,  $F_{4, 32} = 6.609$ ,  $p = 0.0005$ ,  $n = 8, 10, 6, 7, 6$ ). (J, K) Similarly, CSDS-induced depressive-like behaviors were not influenced by NpHR photo-inactivation over BLA→vHPC circuit, but reversed by ChR2 activation over BLA→mPFC circuit (J, social interaction,  $F_{4, 33} = 14.87$ ,  $p < 0.0001$ ,  $n = 10, 8, 6, 7, 7$ ); K, sucrose preference, one-way ANOVA with Welch's

test,  $F_{4, 17.68} = 7.360$ ,  $p = 0.0011$ ,  $\xi P = 0.0605$ .  $n = 9, 8, 6, 7, 7$ ). Most interestingly, The reversal effects of Chr2 activation over one of either BLA pathway on the depressive-like behaviors were not diminished by NpHR photo-inactivation th other BLA pathway, which suggests functional independence of these two BLA projections. Post hoc analysis,  $*p < 0.05$ ,  $**p < 0.01$ ,  $***p < 0.001$ ,  $****p < 0.0001$  compared to control+EYFP group;  $^{\tau}p < 0.1$ ,  $^{\#}p < 0.05$ ,  $^{\#\#}p < 0.01$ ,  $^{\#\#\#}p < 0.001$ ,  $^{\#\#\#\#}p < 0.0001$  compared to CSDS+EYFP group;  $^{\$}p < 0.05$ ,  $^{\$\$}p < 0.01$ ,  $^{\$\$\$}p < 0.001$ ,  $^{\$\$\$\$}p < 0.0001$  compared to CSDS+NpHR (either mPFC or vHPC) group. Data represented as mean  $\pm$  SEM.

#### **Figure 5. Role of mGluR5 in BLA-projection neurons on stress resilience**

(A) Experimental procedures for mGluR5 overexpression with CSDS. (B) Confocal images showing injection sites of LV-EF1a-mGluR5-IRES-ZsGreen1 into the mPFC and vHPC. Scale bars, 500  $\mu$ m. (C, D) mGluR5 overexpression in the mPFC blocked the CSDS-induced social avoidance (C, Kruskal Wallis H test,  $H = 11.65$ ,  $p = 0.0030$ ,  $n = 11, 11, 10$ ) and anhedonic behavior (D, one-way ANOVA with Tukey's test,  $F_{2, 21} = 9.893$ ,  $p = 0.0009$ ,  $n = 8$ ). (E, F) Similarly, mGluR5 overexpression in the vHPC also blocked the CSDS-induced depressive-like behaviors (E, social avoidance: one-way ANOVA with Welch's test,  $F_{2, 17.07} = 11.00$ ,  $p = 0.0009$ ,  $n = 11, 10, 11$ ; F, anhedonic behavior: one-way ANOVA with Tukey's test,  $F_{2, 20} = 4.438$ ,  $p = 0.0254$ ,  $n = 7, 8, 8$ ). (G) Experimental procedures for mGluR5 knockdown in SSDS. (H) Confocal images showing injection sites of AAV5-mGluR5-shRNA into the mPFC and vHPC. Scale bars, 500  $\mu$ m. (I-L) mGluR5 knockdown by infusion of AAV5-hSyn1-mGluR5-shRNA-GFP into the mPFC or vHPC significantly reduced the social interaction (I, mPFC:

one-way ANOVA with Tukey's test,  $F_{2, 29} = 13.97$ ,  $p < 0.001$ ,  $n = 11, 11, 10$ ; K, vHPC: one-way ANOVA with Welch's test,  $F_{2, 22.27} = 9.484$ ,  $p = 0.0010$ ,  $n = 11, 11, 10$ ) and sucrose preference following SSDS (J, mPFC:  $F_{2, 10.23} = 9.424$ ,  $p = 0.0048$ ,  $n = 7, 7, 8$ ; L, vHPC:  $F_{2, 9.286} = 8.871$ ,  $p = 0.0070$ ,  $n = 8$ ). Post hoc analysis,  $*p < 0.05$ ,  $**p < 0.01$ ,  $***p < 0.001$ ,  $****p < 0.0001$  compared to control+ZsGreen1/GFP group;  $^{\#}p < 0.05$ ,  $^{\#\#}p < 0.01$  compared to CSDS/SSDS+ZsGreen1/GFP group. Data represented as mean  $\pm$  SEM.

#### **Figure 6. Distinct signaling pathways downstream to mGluR5 mediating stress resilience**

(A-D) Representative Western blots and quantification of mGluR5, pPKC, tPKC, pERK, tERK, Homer1b/c, pAKT, and tAKT in the mPFC (A, C) and vHPC (B, D) of CTRL, susceptible (SUS), and resilient (RES) mice. (C) mPFC protein levels of mGluR5 were decreased in SUS, but not in RES mice (one-way ANOVA with Tukey's test,  $F_{2, 15} = 18.32$ ,  $p < 0.0001$ ,  $n = 6$ ). Protein levels of Homer1b/c ( $F_{2, 15} = 66.77$ ,  $p < 0.0001$ ,  $n = 6$ ) and pAKT/tAKT (one-way ANOVA with Welch's test,  $F_{2, 6.764} = 163.1$ ,  $p < 0.0001$ ,  $n = 6$ ) also decreased in the mPFC of SUS mice only, whereas pPKC/tPKC and pERK/tERK was not changed (pPKC/tPKC:  $F_{2, 15} = 0.4107$ ,  $p = 0.6704$ ,  $n = 6$ ; pERK/tERK:  $F_{2, 15} = 0.0362$ ,  $p = 0.9645$ ,  $n = 6$ ). (D) In vHPC, protein levels of mGluR5 were also decreased in SUS, but not in RES mice (one-way ANOVA with Tukey's test,  $F_{2, 15} = 33.75$ ,  $p < 0.0001$ ,  $n = 6$ ). In contrast to the mPFC, only SUS animals showed reduced protein levels of pPKC/tPKC ( $F_{2, 15} = 7.204$ ,  $p = 0.0064$ ,  $n = 6$ ) and of pERK/tERK ( $F_{2, 15} = 9.444$ ,  $p = 0.0022$ ,  $n = 6$ ), but no changes in protein levels of Homer1b/c ( $F_{2, 15} = 1.178$ ,  $p = 0.3349$ ,  $n = 6$ ) and pAKT/tAKT (Kruskal Wallis H test,  $H = 3.193$ ,  $p = 0.2128$ ,  $n = 6$ ). Post hoc analysis,  $*p < 0.05$ ,  $**p < 0.01$ ,  $***p < 0.001$ ,  $****p < 0.0001$

compared to control group;  $^{\#}p < 0.05$ ,  $^{\#\#}p < 0.01$ ,  $^{\#\#\#}p < 0.0001$  compared to SUS group. (E)  
 Experimental procedures for pharmacological inhibition of mGluR5 signals during SSDS. (F)  
 Representative images of cannula implant sites in the mPFC and vHPC. Scale bars, 1 mm. (G,  
 H) Infusion of LY294002 into the mPFC significantly reduced social interaction (G, one-way  
 ANOVA with Welch's test,  $F_{3, 56.48} = 7.360$ ,  $p = 0.0003$ ,  $n = 19, 17, 18, 18$ ) and sucrose  
 preference (H, one-way ANOVA with Tukey's test,  $F_{3, 26} = 17.62$ ,  $p < 0.0001$ ,  $n = 8, 7, 7, 8$ )  
 after SSDS, but U012 did not. (I, J) However, infusion of U012 into the vHPC induced social  
 avoidance (I, Kruskal Wallis H test,  $H = 15.19$ ,  $p = 0.017$ ,  $n = 15$ ) and anhedonic behavior (J,  
 one-way ANOVA with Tukey's test,  $F_{3, 27} = 4.572$ ,  $p = 0.0103$ ,  $n = 8, 8, 7, 8$ ) after SSDS, but  
 LY294002 did not. Post hoc analysis,  $^*p < 0.05$ ,  $^{***}p < 0.001$ ,  $^{****}p < 0.0001$  compared to  
 control+Vehicle group.;  $^{\#}p < 0.05$ ,  $^{\#\#}p < 0.01$ ,  $^{\#\#\#}p < 0.001$  compared to SSDS+Vehicle group;  
 $^{\$}p < 0.05$ ,  $^{\$\$}p < 0.01$ ,  $^{\$ \$ \$}p < 0.001$  compared to SSDS+LY294002 group. Data represented as  
 mean  $\pm$  SEM.

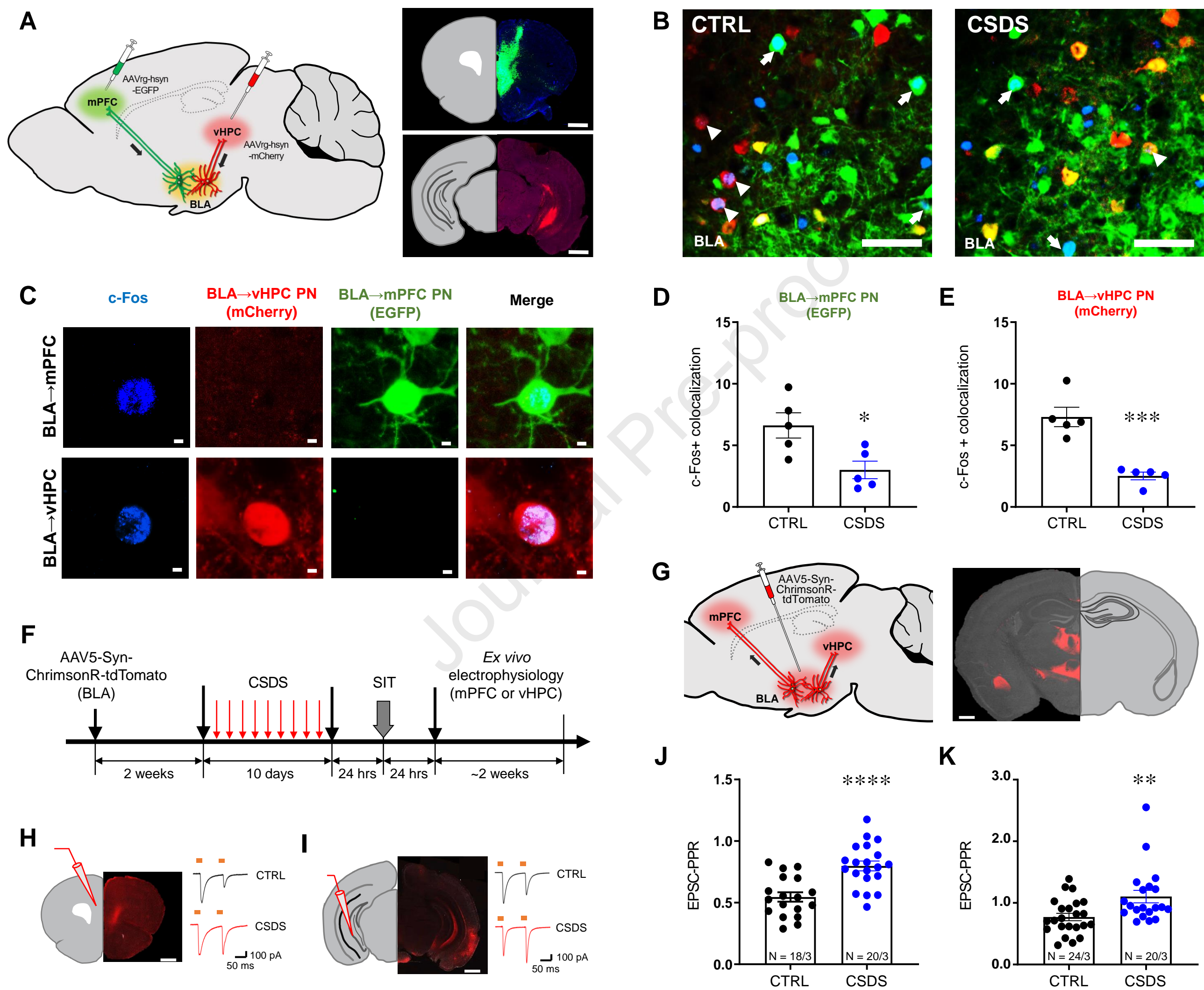


Figure. 2

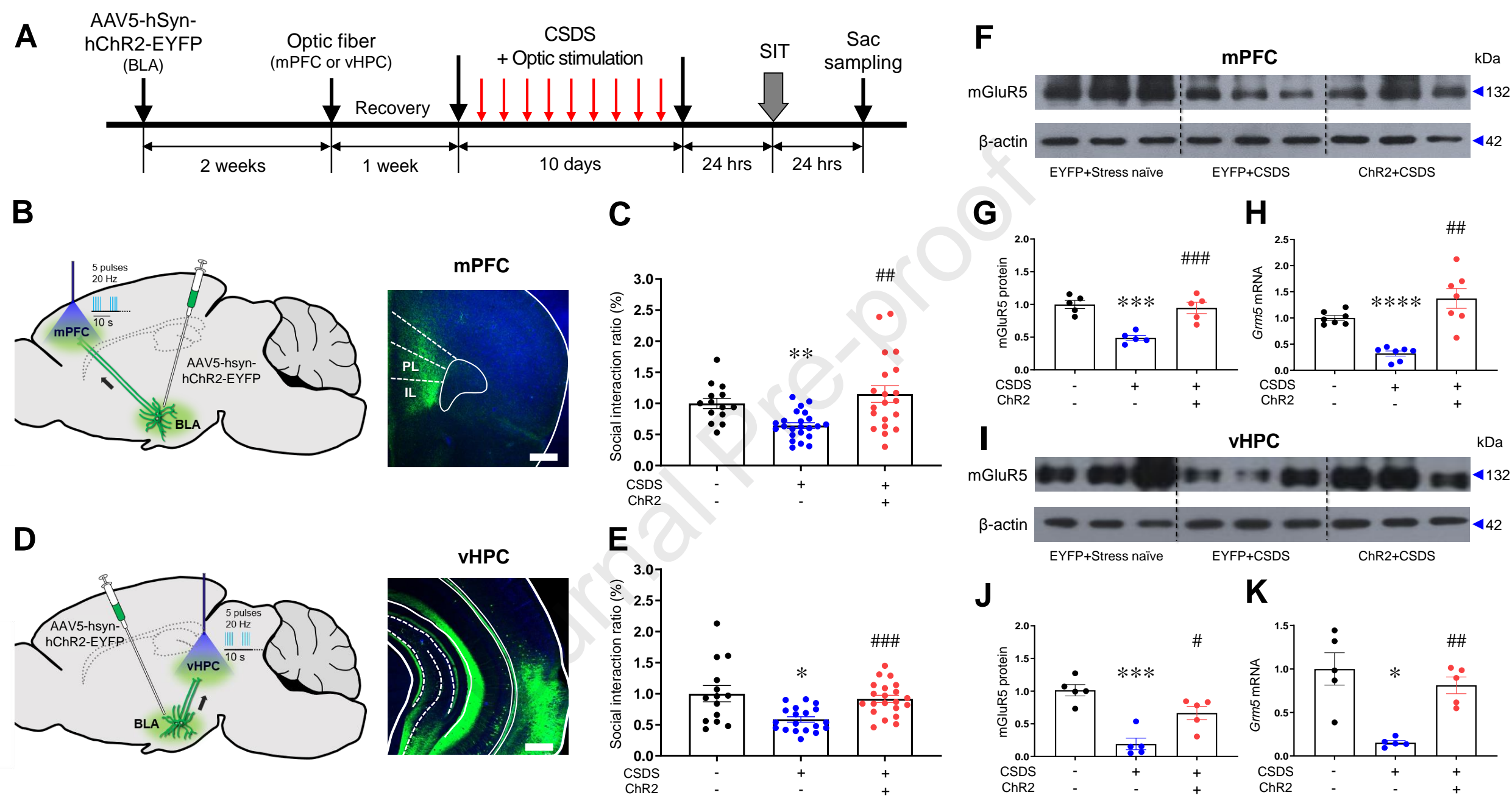


Figure. 3

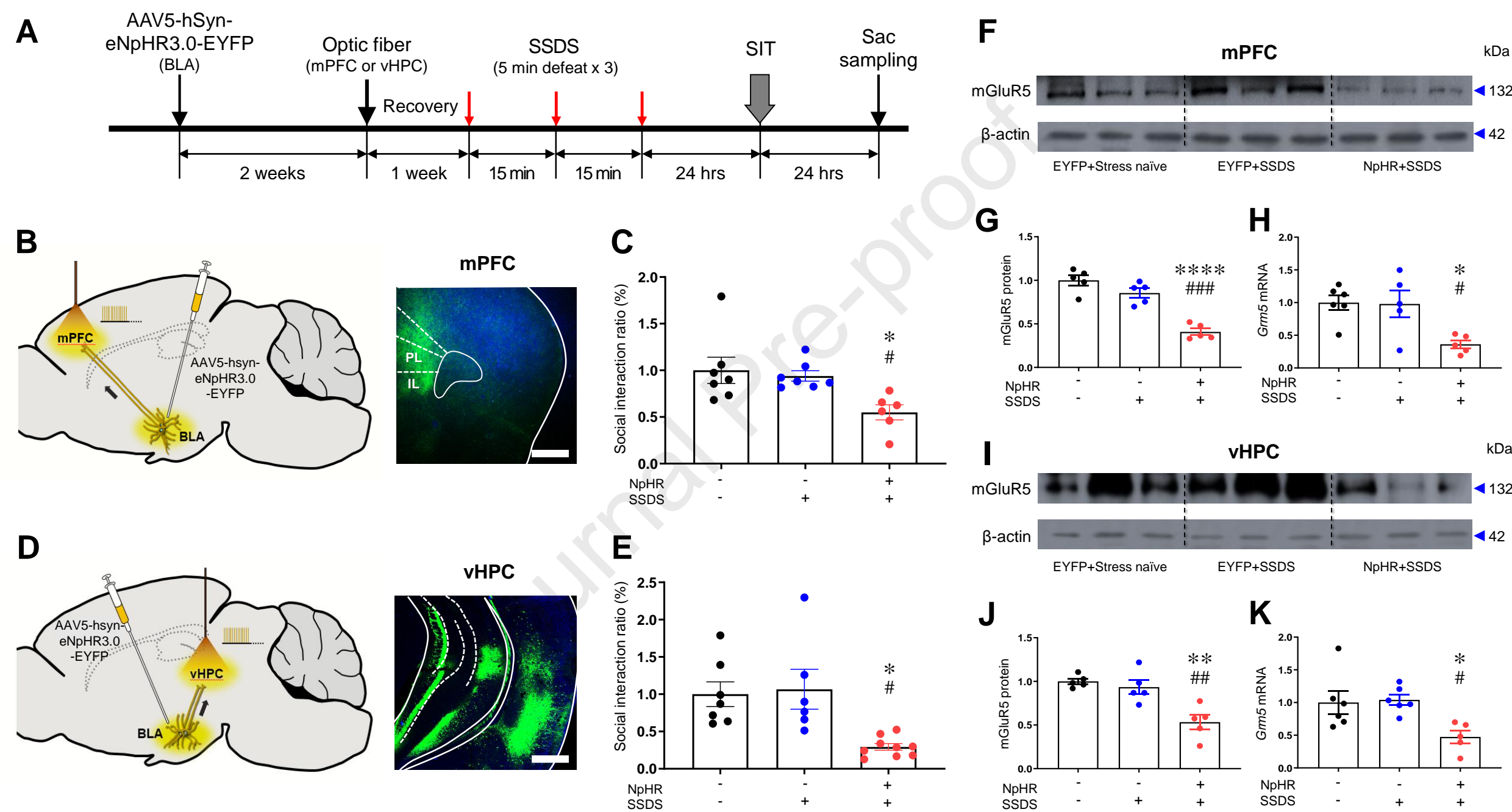
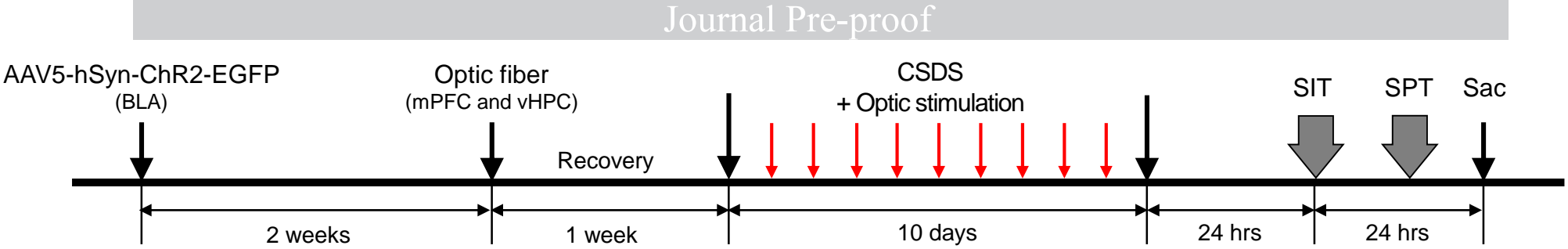
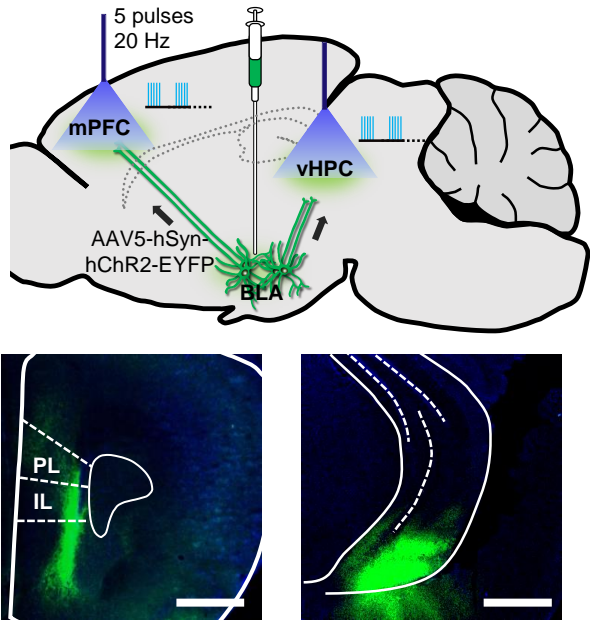


Figure. 4

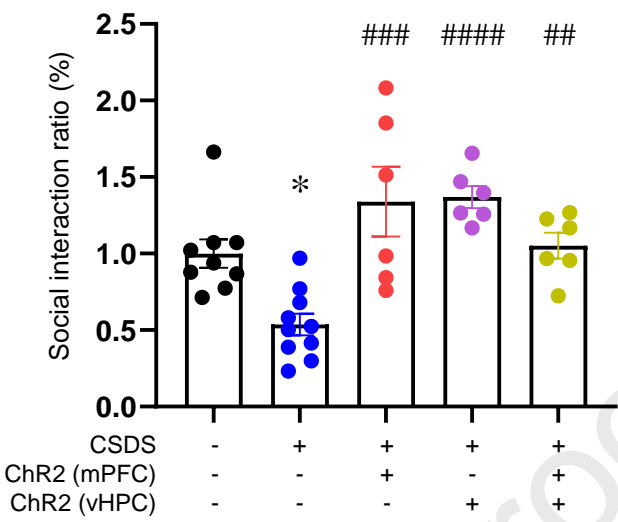
A



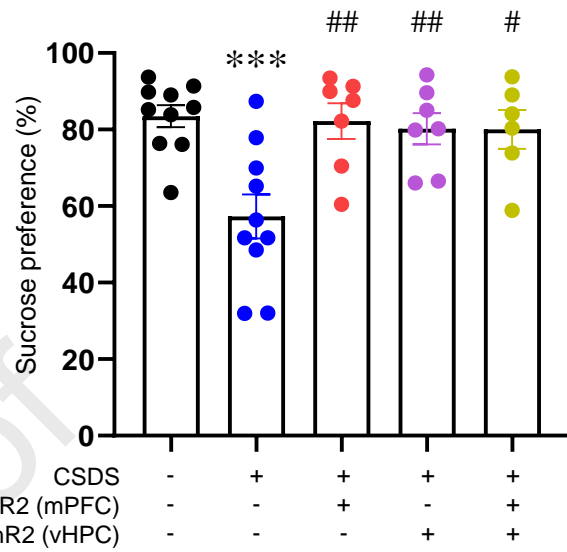
B



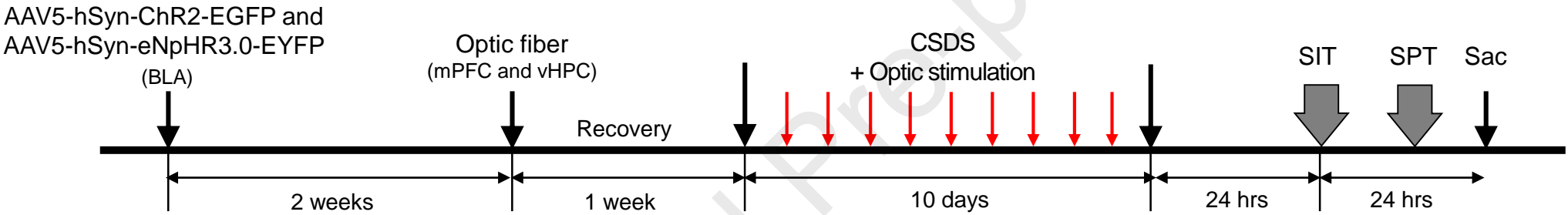
C



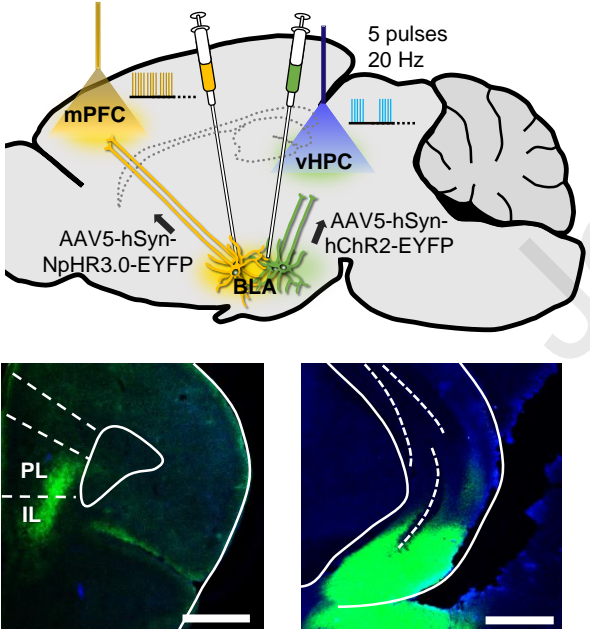
D



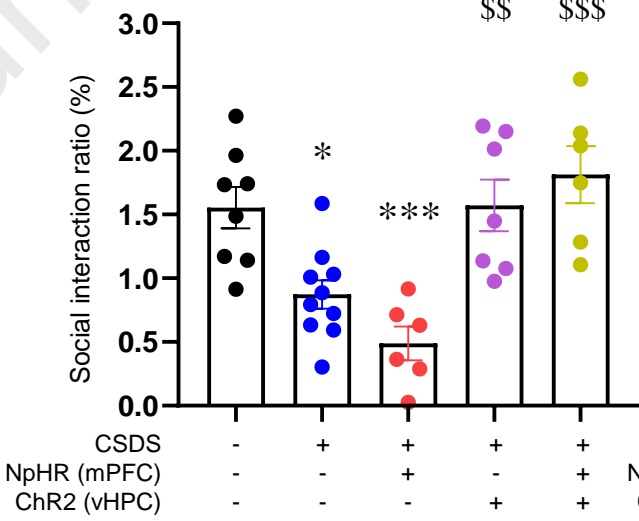
E



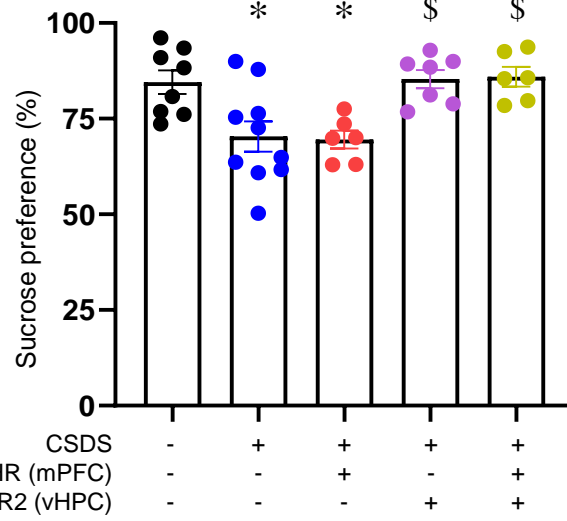
F



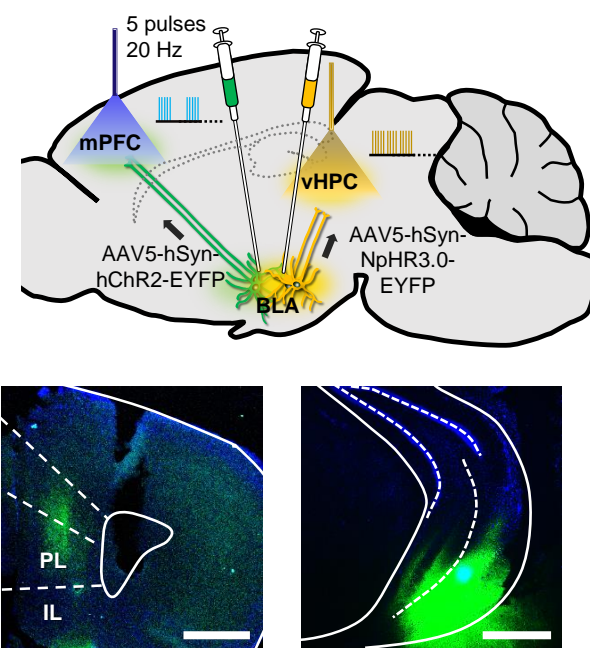
G



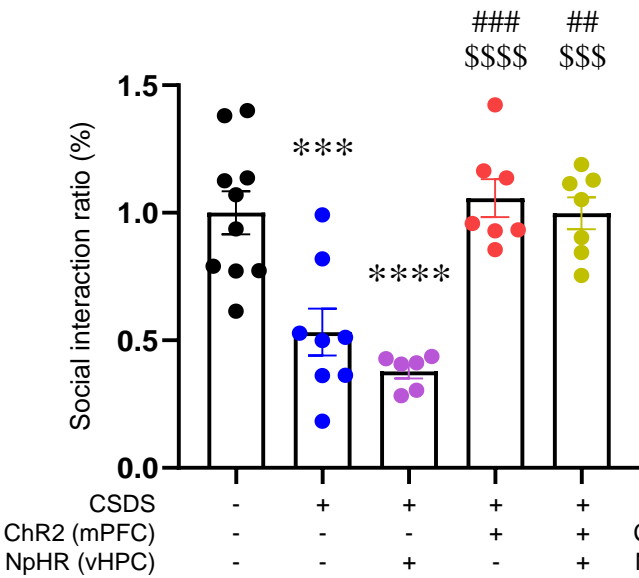
H



I



J



K

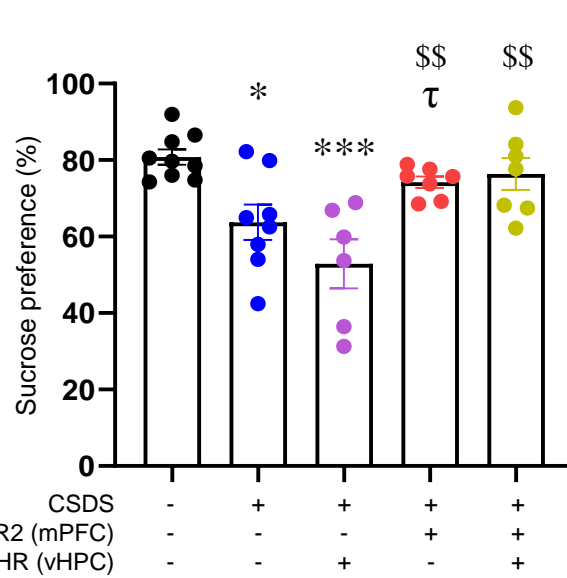


Figure. 5

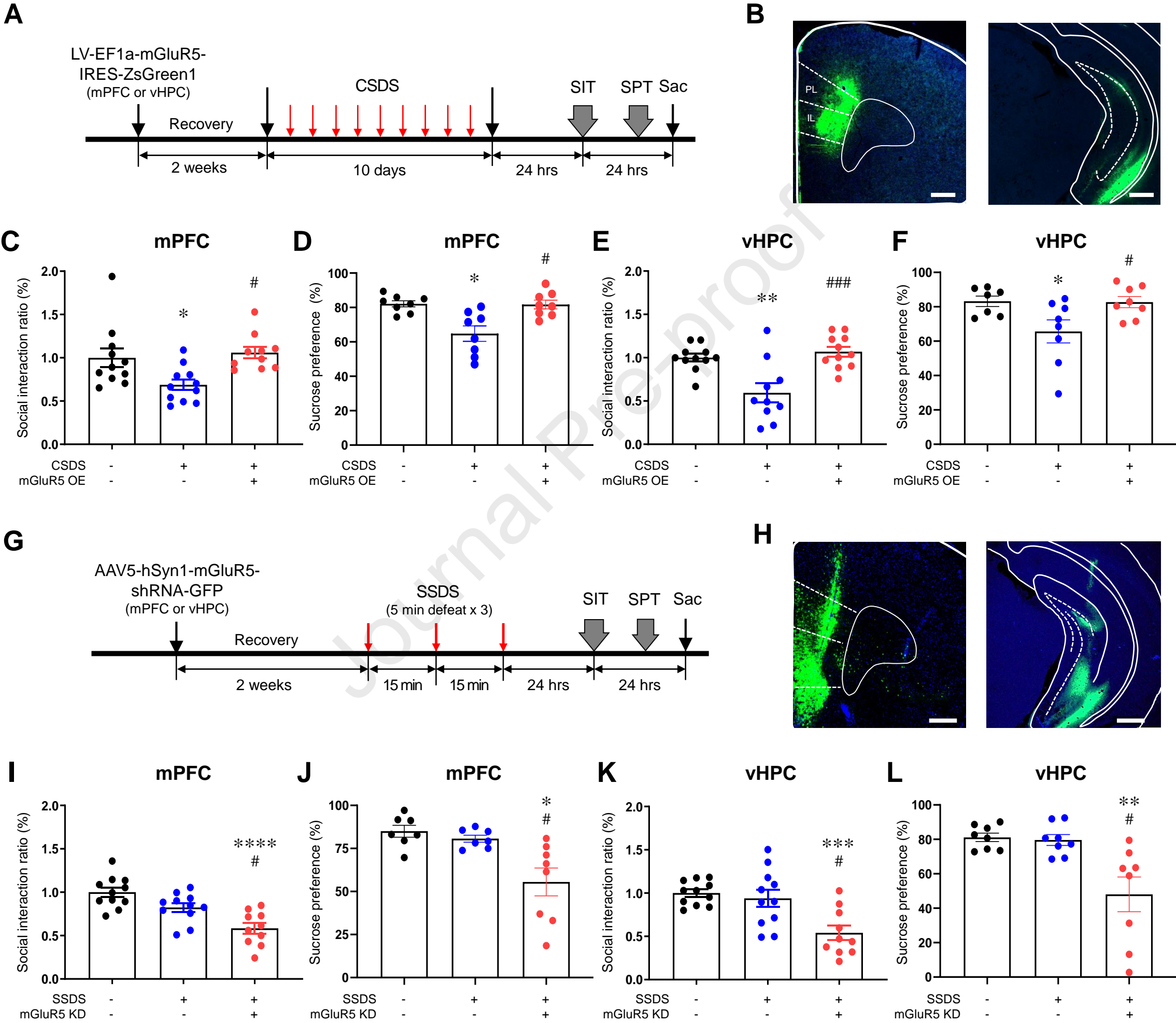


Figure. 6

